

Effect of Process Parameters on Gasification: Review

Isam Janajreh
Masdar Institute
ijanajreh@masdar.ac.ae

Idowu Adeyemi
Masdar Institute
iadeyemi@masdar.ac.ae

Abstract

Gasification is receiving much attention, and the renaissance is attributed to its added efficiency when used in the integration combined cycle and its environmental advantage in converting any waste organic material into a clean syngas. Although many studies have been conducted on gasification in the past, these works are mostly scattered, and it is hard to keep track of the information. A novel and comprehensive approach for the review of the literature on gasification is presented in this work, seeking to streamline the information in an attempt to determine the optimal gasification process conditions. Progress on feedstock properties of various fuels for gasification to foresee their potentiality for the process is also reported in this paper, including reviews of gasification processes and various classifications and technologies and the effect of various process parameters like pressure, temperature, and catalyst on gas composition and efficiency of gasifiers.

Introduction

Environmental concerns are alerting the world to the imminent dangers of overdependence on fossil fuels as the drivers of industrialization, transportation, and other daily activities. Global warming has steadily emerged from the realm of speculative science to the reality of definitive global concern in the form of rising water levels with consequent flooding and weather vagaries. In 2002, for the first time in recorded history, a 12,000-year-old ice shelf the size of Luxembourg came adrift from the Antarctic and melted in just 35 days [1]. The glaciers of Africa's Kilimanjaro and the tropical Andes in South America are melting so fast that experts believe they could disappear within the next 20 years [2]. In addition to this, world energy demand is rising sharply, and it is believed that the world's energy reserves could be depleted in few decades. These uncontested facts are alarming and make the switch to continuous and environmental friendly energy sources and technologies more urgent. Biomass is one of the choices of renewable energy sources that is now getting more attention, since the people are gaining more knowledge about the issue of sustainable energy and production. Although many options are available to convert biomass to useful energy, this study only considers the thermochemical pathway.

There are three pathways of thermochemical conversion: pyrolysis, gasification, and combustion. Gasification involves the conversion of carbonaceous materials into synthetic gases in the presence of a limited amount of oxidation or oxidizing agent. The synthetic gas produced leaves the reactor with pollutants and therefore requires cleaning to satisfy engine

requirements. Mixed with air, the cleaned synthetic gas can be used in an integrated gasification combined cycle (IGCC), where a combination of gas turbine, which is powered by the cleaned synthetic gas, and a steam turbine that utilizes the waste heat from the gas turbine, would further increase the efficiency of the turbine. This work focuses on reviewing the central process in the IGCC operation to keep track of the numerous findings of studies in this area.

Feedstock Properties

Feedstocks for gasification are composed of majorly moisture, volatile matter, fixed carbon, and ash. A detailed analysis of these feedstocks has to be provided before gasification occurs. Two ASTM standards (D5142 and D5291) are carried out utilizing TGA and Flash elemental analyzer to determine these compositions. Results are presented in volume reduction versus temperature (or time) of the dynamic heating as illustrated in Figure 1 for Kentucky sub-bituminous coal.

In general, moisture and ash are inversely proportional to the feedstock exergy thereby affecting gasification process efficiency. This analysis not only helps to foresee the potential of the feedstock as a good fuel for gasification but also helps in the proper selection of sub-models for numerical analysis. Various characterization techniques have been used in the past for this purpose. Raveendran et al. [4] obtained the composition of 13 biomasses via ultimate and proximate analysis. The results of his study are reported in Table 1.

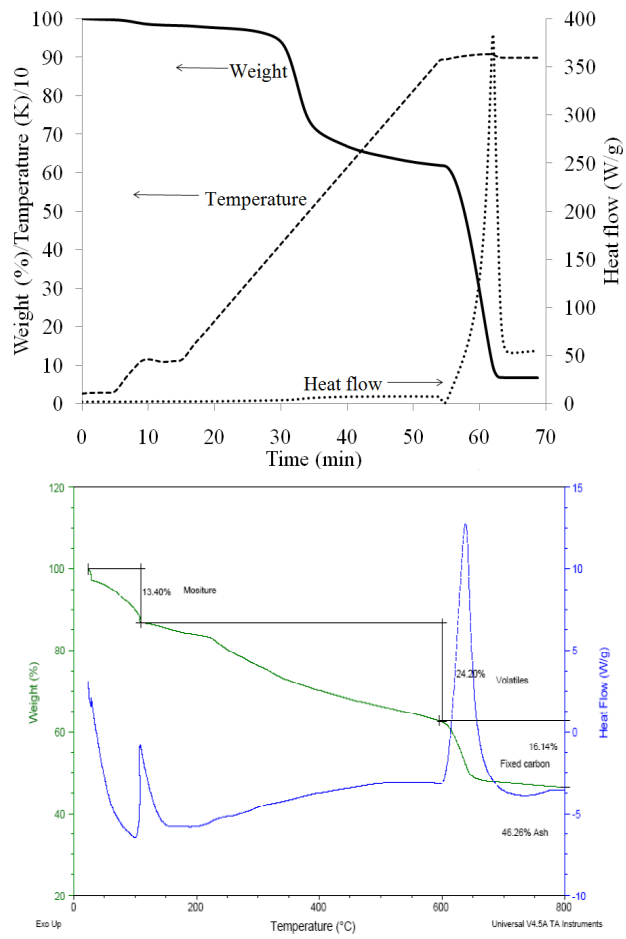


Figure 1. DSC/TGA curve of RTC-coal and Ulva macroalgae with respect to time and temperature

Table 1. Proximate and ultimate analysis of biomasses [4]

Sl. no.	Biomass	VM (daf) (%)	Ash (db) (%)	Fixed carbon (100-VM) (%)
1	Bagasse	84.2	2.9	15.8
2	Coconut coir	82.8	0.9	17.2
3	Coconut shell	80.2	0.7	19.8
4	Coir pith	73.3	7.1	26.7
5	Corn cob	85.4	2.8	14.6
6	Corn stalks	80.1	6.8	19.9
7	Cotton gin waste	88.0	5.4	12.0
8	Groundnut shell	83.0	5.9	17.0
9	Millet husk	80.7	18.1	19.3
10	Rice husk	81.6	23.5	18.4
11	Rice straw	80.2	19.8	19.8
12	Subabul wood	85.6	0.9	14.4
13	Wheat straw	83.9	11.2	16.1

Sl. no.	Biomass	Ultimate analysis (wt%)				HHV ^a (MJ/kg)	Density (kg/m ³)	x	y	z	Percentage conversion of carbon
		C	H	N	O						
1	Bagasse	43.8	5.8	0.4	47.1	16.29	111	3.65	5.8	2.94	81
2	Coconut coir	47.6	5.7	0.2	45.6	14.67	151	3.97	5.7	2.85	72
3	Coconut shell	50.2	5.7	0.0	43.4	20.50	661	4.18	5.7	2.71	65
4	Coir pith	44.0	4.7	0.7	43.4	18.07	94	3.67	4.7	2.71	74
5	Corn cob	47.6	5.0	0.0	44.6	15.65	188	3.97	5.0	2.79	70
6	Corn stalks	41.9	5.3	0.0	46.0	16.54	129	3.49	5.3	2.88	82.3
7	Cotton gin waste	42.7	6.0	0.1	49.5	17.48	109	3.56	6.0	3.10	87
8	Ground nut shell	48.3	5.7	0.8	39.4	18.65	299	4.03	5.7	2.46	61.2
9	Millet husk	42.7	6.0	0.1	33.0	17.48	201	3.56	6.0	2.063	58
10	Rice husk	38.9	5.1	0.6	32.0	15.29	617	3.24	5.1	2.0	62
11	Rice straw	36.9	5.0	0.4	37.9	16.78	259	3.08	5.0	2.37	82.4
12	Subabul wood	48.2	5.9	0.0	45.1	19.78	259	4.02	5.9	2.82	70.2
13	Wheat straw	47.5	5.4	0.1	35.8	17.99	222	3.96	5.4	2.24	56.5
Average		44.6	5.5	0.3	41.8	17.32	253.84	3.72	5.49	2.61	70.89

^aHigher heating value.

In another work, Talab et al. [5] reported the characterization of pine needles, plywood, particle, oil shale, raw horse manure, and tires using TGA and Flash elemental analyzer as shown in Table 2.

Table 2. Proximate and ultimate analysis of feedstocks [5]

Material	Pine needles	Plywood	Coal	Oil shale	Raw horse manure	Tires
Moisture%	9.013	9.706	2.304	1.82	62.13	0.7127
Volatile%	44.58	56.39	30.19	21.21	16.7	61.21
Fixed carbon%	42.28	31.46	57.2	13.7	8.389	30.04
Ash%	4.127	2.44	10.306	63.27	12.781	8.0373

No.	Feedstock	wt% N	wt% C	wt% H	wt% S	wt% O
1	Bituminous coal	1.752	58.560	4.986	0.463	-
2	RTC coal	2.197	72.302	4.956	0.997	7.924
3	Massey coal	1.987	66.939	4.638	1.165	11.271
4	Oil shale (Jordan)	0.412	20.332	2.087	3.382	15.283
5	Pine needle (India)	1.432	46.879	6.075	0.000	42.105
6	Virgin polymer	0.044	84.942	14.454	0.000	0.235
7	Waste polymer	0.048	83.648	14.165	0.000	0.417
8	Horse manure	2.160	39.700	5.565	0.135	-
9	Ply-wood	0.393	49.590	6.280	0.000	43.740
10	Tire	0.290	80.060	7.570	1.360	10.720
11	Petroleum coke	2.780	88.480	3.930	4.770	0.040

Another means of characterizing materials for gasification is through using the Van Krevelen diagram, where the heating value, atomic H/C, and O/C ratio can easily be deduced. The O/C ratio is particularly important for proper determining the correct equivalence ratio for the gasification process. The Van Krevelen diagram and the distribution of the different feedstocks are depicted in Figure 2.

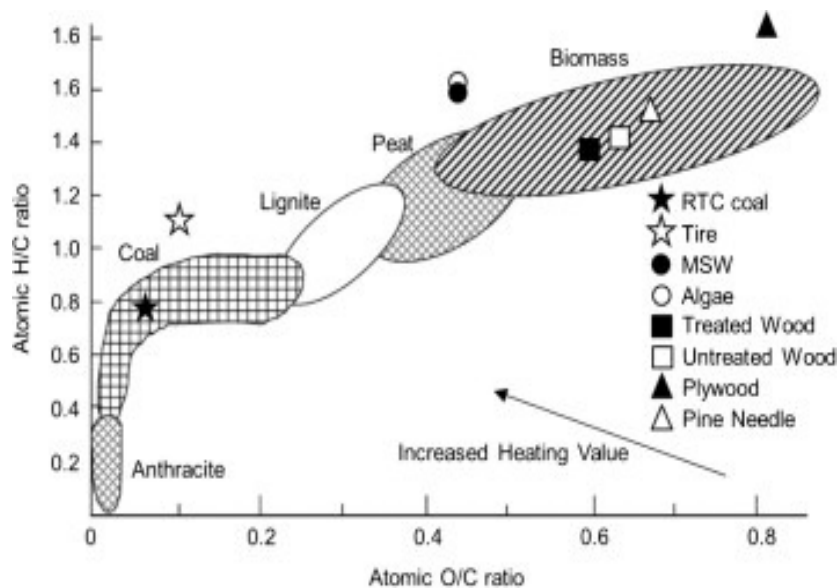


Figure 2. The Van Krevelen diagram [3]

During material characterization, the weight percent of each feedstock is used to calculate the empirical formula by considering only carbon, hydrogen, oxygen, and nitrogen. Table 3 shows the empirical formula corresponding to each feedstock. These formulas are calculated on molar bases by normalizing through a single atom of carbon. The higher heating values (HHV), as shown in Table 3, are calculated using the proximate or ultimate analysis bases as follows [17]:

$$HHV \left(\frac{MJ}{Kg} \right) = 0.3491 C + 1.1783 H - 0.1043 O \quad \text{or} \quad (1.a)$$

$$HHV \left(\frac{MJ}{Kg} \right) = -0.11 (\text{Moisture}) + 0.33 (\text{Vol})0.35 (\text{Carbon}) - 0.03 (\text{AsH}) \quad (1.b)$$

where C, H and O are the corresponding weight percentage of carbon, hydrogen, and oxygen present in each feedstock. The results show that for the solid feedstock the coal has the highest HHV while pine needles and plywood have similar HHVs.

Table 3. Empirical formula and heating value (HHV) of feedstock

Feedstock	Empirical formula	HHV KJ/Kmole	HHV MJ/Kg
RTC coal	$CH_{0.7946}O_{0.0670}N_{0.0260}$	502928	34.38
Pine needles	$CH_{1.5550}O_{0.6736}N_{0.0261}$	489784	19.83
Ply-wood	$CH_{1.5196}O_{0.6615}N_{0.0067}$	487566	20.14
Lignite	$CH_{0.8450}O_{0.2912}N_{0.0268}$	469939	26.28
Waste cooking oil	$C_{54}H_{105}O_6$	743176	41.56

Gasification Process

Gasification is a thermochemical conversion process whereby carbonaceous materials (coal particle, oil shale, tire crumbs, municipal solid waste, etc.) undergo partial oxidation at a considerably high temperature to yield synthetic gases containing mainly carbon monoxide and hydrogen. During gasification, the carbonaceous matter is fed into a high-temperature pressurized container along with steam or carbon dioxide and a substoichiometric amount of oxygen, which is converted to combustible gases (mixture of CO, CH₄, and H₂), with char, water, and condensable tar as minor products. In the first step, pyrolysis, the organic matter is decomposed by heat into gaseous and liquid volatile materials and char (mainly a nonvolatile material, containing high carbon content). In the second step, the hot char reacts with the gases (mainly CO₂ and H₂O), leading to product gases: CO, H₂ and CH₄ [7]. The producer gas leaves the reactor with pollutants and therefore requires cleaning to satisfy engine requirements. Mixed with air, the cleaned producer gas can be used in IGCC, gas turbines (in large-scale plants), gas engines, gasoline, or diesel engines. Producer gas is a mixture of carbon monoxide, hydrogen, and methane, together with carbon dioxide, nitrogen, and other incombustible gases [8]. The reaction sequence for gasification is as depicted in Figure 3.

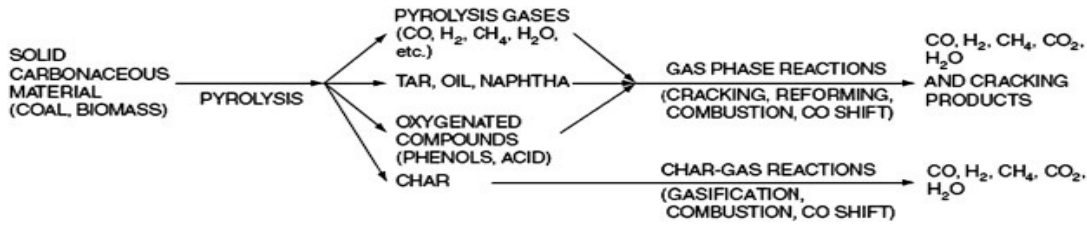


Figure 3. Reaction sequence for gasification of particle and biomass adapted from Higman and Van der Burgt [6]

In a wide sense, the gasification process can be classified into the following stages [9-12], which occur consecutively:

Drying

In this stage, the moisture content of the biomass is reduced. Typically, the moisture content of biomass varies from 5% to 40%. Drying occurs at about 100–200°C with a reduction in the moisture content of the biomass to less than 2%. This step can be subdivided into two; the primary step is inert heating, whereby the feedstock particles reach the allotted moisture temperature to evaporate and release.

Devolatilization (Pyrolysis)

This is essentially the thermal decomposition of the biomass in the absence of oxygen or air. In this process, the volatile matter in the biomass is reduced. This results in the release of hydrocarbon gases from the biomass, which reduce the biomass to solid charcoal. The hydrocarbon gases can condense at a sufficiently low temperature to generate liquid tars.

Oxidation

This is a reaction between solid carbonized biomass and oxygen in the air, resulting in formation of CO₂. Hydrogen present in the biomass is also oxidized to generate water. A large amount of heat is released with the oxidation of carbon and hydrogen. If oxygen is present in sub-stoichiometric quantities, partial oxidation of carbon may occur, resulting in the generation of carbon monoxide.

Reduction

In the absence (or sub-stoichiometric presence) of oxygen, several reduction reactions occur in the 800-1000°C temperature range. These reactions are mostly endothermic. The main reactions in this category are the water-gas, Boudouard, shift, and methane.

Gasification Classifications and Technologies

Gasification can be classified in several ways [13]: by the agent, such as air-blown, oxygen-blown, or steam gasifiers; by heat source, either auto-thermal or direct (heat is provided by partial combustion of biomass) and allothermal or indirect gasifiers (heat is supplied by an external source via a heat exchanger or an indirect process, i.e., solar or plasma gasification); by the gasifier pressure, atmospheric or pressurized. The fourth and most common is by the reactor design and that follows three main subcategories: high temperature entrained flow, fixed bed (sometimes referred to as moving bed), and fluidized bed gasifiers. More details on each of these designs are given below.

Fixed (or Moving) Bed Gasifiers

Moving bed gasifiers are countercurrent flow reactors in which the particle enters at the top of the reactor and air or oxygen enters at the bottom. As the particle slowly moves down through the reactor, it is gasified and the remaining ash drops out of the bottom of the reactor. Because of the countercurrent flow arrangement, the heat of reaction from the gasification reactions serves to pre-heat the particle before it enters the gasification reaction zone. Consequently, the temperature of the syngas exiting the gasifier is significantly lower than the temperature needed for complete conversion of the particle. Fixed bed gasifiers are simple to construct and generally operate with high carbon conversion, long feedstock residence time, low gas velocity, and low ash carry-over [14, 15].

Fluidized Bed Gasifiers

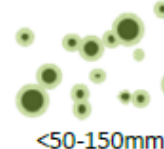
A fluidized bed gasifier is a back-mixed or well-stirred reactor in which there is a consistent mixture of new particle particles mixed in with older, partially gasified and fully gasified particles. The mixing also fosters uniform temperatures throughout the bed. The flow of gas into the reactor (oxidant, steam, recycled syngas) must be sufficient to float the particles within the bed but not so high as to entrain them out of the bed. However, as the particles are gasified, they will become smaller and lighter and will be entrained out of the reactor. It is important that the temperatures within the bed are less than the initial ash fusion temperature of the particle to avoid particle agglomeration. These gasifiers are characterized by short residence time, high temperatures, high pressures, and large capacities [16].

Entrained Flow Gasifiers

A finely ground particle is injected in concurrent flow with the oxidant. The particle rapidly heats up and reacts with the oxidant. The residence time of an entrained flow gasifier is seconds to several seconds. Because of the short residence time, entrained flow gasifiers must operate at high temperatures to achieve high carbon conversion. Consequently, most entrained flow gasifiers use oxygen rather than air and operate above the slagging temperature of the particle.

The size requirements, configuration, and the effect of the different gasifier technologies on the gas composition are presented in Figure 4 and Tables 4 and 5.

Table 4. Feedstock requirements for different types of gasifiers [17]

Gasifier	Size	Moisture	Composition	Other
EF	 <1mm	15%	Should not change over time. Limited proportion of high-ash agricultural residues	Pre-treatment steps being used
BFB (and Dual with BFB gasifier)	 <50-150mm	10-55%	Can change over time Care needed with some agricultural residues	
CFB (and Dual with CFB gasifier)	 <20mm	5-60%	Can change over time Care needed with some agricultural residues	
Plasma	 Not important	Not important	Not important, can change over time. Higher energy content feedstocks preferred	Used for a variety of different wastes, gate fees common

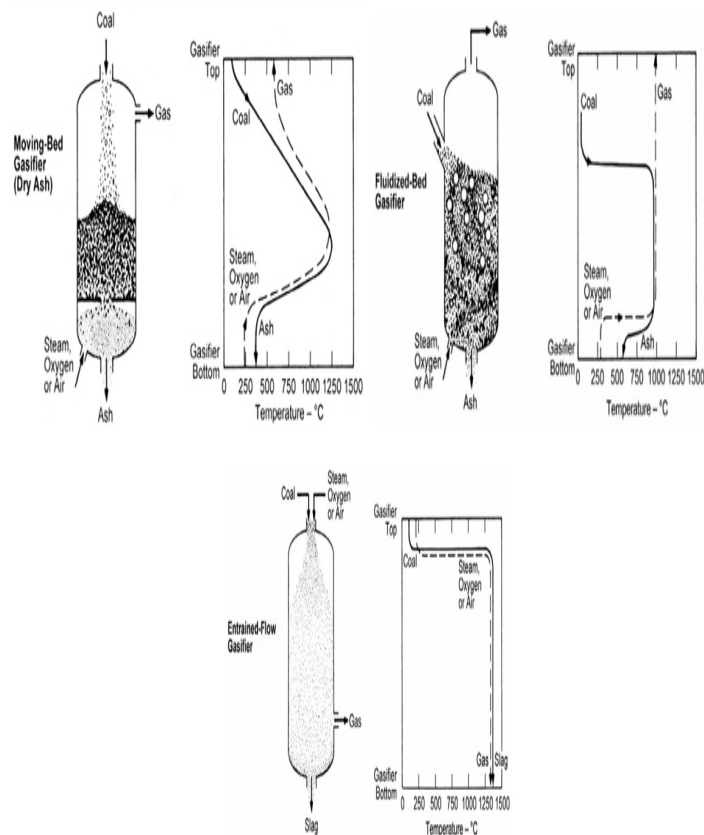


Figure 4. Moving bed (left), fluidized bed (right) and entrained flow (center) gasifiers [18]

Effect of Process Conditions on Gasification

Effect of Pressure

Roberts et al. [31] studied the effects of high pressure and heating rate during coal pyrolysis on char gasification reactivity of three Australian coals. Their results indicate that effects of pyrolysis pressure and heating rate on char gasification rates are more likely to be due to effects of structure and surface area and (depending on reaction conditions) the consequent effects on diffusion of reactants to the char surface, rather than on the intrinsic reactivity of the coal chars. Young [32] reported the effects of pressure on black liquor gasification and deduced that increasing pressure decreased the porosity of pyrolysis chars. Tülay et al. [33] studied the simultaneous effects of temperature and pressure on catalytic hydrothermal

Gasifier Feeding	Oxidant	H ₂	CO	H ₂ :CO ratio	CO ₂	H ₂ O	Methane	Hydro- carbons (C _n)	Nitrogen (N ₂)	HCN, NH ₃ , NO _x	Sulphur (COS, H ₂ S, CS ₂)	Halides (HCl, Br, F)
Direct	O ₂	37.2%	36.4%	1.02	18.9%	7.5%	0.06%		0.1%			
Direct	O ₂	23%	43%	0.53	11%	<0.1%			5%	HCN 3.4mg/Nm ³ NH ₃ 0.4mg/Nm ³		1.7mg/Nm ³
Direct	O ₂ /Steam	20%	22%	0.91	?	5%						
Direct	O ₂	37.5%	40%	0.94	15%	3%	<1%		3%			
Direct	Air	6-12%	14-15%	0.4-0.8	16-17%	3-4%	2.9-4.1%		36-58%			
Direct	Air	16.0%	21.5%	0.74	10.5%	?			46.5%			
Direct	Air	11%	16%	0.69	10.5%	12%	Methane & C ₂ , 6.5%		44%			
Direct	O ₂ /Steam	31.6%	22.0%	1.44	33.6%		C ₂ H ₆ 0.6%, C ₂ H ₄ 1.2%		3%			
Direct	Air	18%	14%	1.29	16%	10%	3%		39%			
Direct	O ₂ /Steam	30.1%	33.1%	0.91	30.6%		C ₂ H ₆ 770ppm		0.4%	90ppm NH ₃	H ₂ S 0.03%	Oppm HCl
Direct	Air	18%	16%	1.13	16%		5.5%	2.38%	42%	NH ₃ 2,200mg /Nm ³	H ₂ S 150mg /Nm ³	HCl 150mg /Nm ³
Indirect	Steam	51.5%	24.1%	2.14	17.8%		5.8%		0.5%			
Indirect	Steam	26%	39%	0.67	18%		11%					
Indirect	Steam	43.5%	39.2%	4.71	28%	3.6%	4.7%	5%		0%		
Indirect	Steam	38-45%	23-25%	1.6-1.8	20-23%		9-12%	C ₂ H ₆ 2-3%, C ₂ H ₄ 0.5%, C ₂ H ₂ 0.2%	2-3%	1000- 2000ppm NH ₃	H ₂ S 40- 70ppm, other 30ppm	
Indirect	Steam	22%	44.4%	0.50	12.2%		15.6%	C ₂ H ₆ 5.1%				
Indirect	Steam	18.0%	44.0%	0.41	11.0%	25			1.0%	NH ₃ 500-1000 ppm	H ₂ S 40- 100ppm	
Direct	None	15.0%	40.4%	0.30	3.6%	37						

Table 5. Composition of gasification technology [30]

gasification of glucose. The yield of hydrogen among gaseous products was reported to increase with increasing temperature and decreasing pressure. Sharma [34] examined the effect of steam partial pressure on gasification rate and gas composition of product gas from catalytic steam gasification of hyper-coal, while Malekshahian [35] worked on the effect of pressure on gasification of petroleum coke with carbon dioxide. The surface characterization of pet-coke during gasification at different pressures showed that the surface area increased with pressure, accounting for most, but not all, of the increase in the reaction rate.

Wall et al. [36] studied the effects of pressure on coal reactions during pulverized coal combustion and gasification. The pressure has been found to significantly influence the volatiles' yield and coal swelling during devolatilization, hence the structure and morphology of the char generated. More char particles of high porosity are formed at higher pressures. Cetin et al. [37] explored the effect of pyrolysis pressure and heating rate on radiata pine char structure and apparent gasification reactivity. Pyrolysis pressure, in particular, was found to influence the size and the shape of char particles while high heating rates led to plastic deformation of particles (melting) resulting in smooth surfaces and large cavities. Zhang et al. [38] studied the effect of CO₂, partial pressure on gasification reactivity. As CO₂ partial pressure decreases, the formation rate of surface complexes becomes comparable to the desorption rates, and the reaction rate begins to deviate from desorption rate-controlled.

Effect of Catalyst

Studies of the effects of catalysts on gasification has focused primarily on three distinct groups of catalysts for biomass gasification and are described below [39]:

Dolomite Catalyst. The use of dolomite as a catalyst in biomass gasification has attracted much attention [40-55], since it is cheap, disposable, and can significantly reduce the tar content of the product gas from a gasifier. It may be used as a primary catalyst, dry-mixed with the biomass or, more commonly, in a downstream reactor, in which case it is often referred to as a guard bed [39]. The chemical composition of dolomite varies from source to source but it generally contains 30 wt. % CaO, 21 wt. % MgO, and 45 wt. % CO₂; it also contains the trace minerals SiO₂, Fe₂O₃ and Al₂O₃. Orio et al. [40] investigated four different dolomites from Norte, Chilches, Malaga and Sevilla for oxygen/steam gasification of wood in a downstream catalytic reactor. The gas yields were increased by the catalyst for all of the dolomites. The order of activity was Norte>Chilches>Malaga>Sevilla. Aznar et al. [43, 53] also investigated the use of Malaga dolomite for steam/oxygen gasification. They reported that the H₂ content of the flue gas increased by 7 vol. %, while the CO content decreased by 7 vol. %. Ekstrom et al. [55] also achieved almost 100% conversion of tar at 700–800° C using Malaga dolomite under steam reforming conditions. However, they also observed a marked increase in CH₄ and C₂H₄ at lower temperatures and showed that calcined dolomite was 10 times more active than the uncalcined material [55], in agreement with the results of several authors [40-43, 53]. Delgado et al. [41] investigated the use of Norte dolomite and compared it with calcite CaO and magnesite MgO for the steam reforming of biomass tars. Alden et al. [48] and Lammers et al. [54] examined the catalytic reforming of naphthalene over dolomite. The former [48] reported that the degree of conversion of naphthalene when passed over calcined dolomite at 800° C varied with the composition of the carrier gas.

Alkali Metal and Other Metallic Catalysts. Alkali metal catalysts for the elimination of tar and up-grading of the product gas have also been investigated by several groups [56-64]. Mudge et al. [56] studied the catalytic steam gasification of wood using alkali carbonates and naturally occurring minerals, which were either impregnated or mixed with the biomass. DeGroot and Shafizadeh [62] reported that the activation energy for uncatalysed steam gasification of wood was 258.1 kJ/mol and the activation energy for K₂CO₃ catalysed wood gasification was 178.6 kJ/mol [62]. Gebhard et al. [64] investigated a catalyst specifically designed for tar destruction.

Nickel Catalyst. The most significant body of literature published on the area of hot gas cleaning for biomass gasification concerns nickel catalysts [40, 64-79]. Several groups [40, 54-56, 64] have investigated a system of raw gas cleaning that involves a dolomite or alkali catalyst for the removal of tar up to 95% followed by the adjustment of the gas composition using a nickel steam reforming catalyst. Baker et al. [67-69] investigated several commercial nickel catalysts and have compared them with specially prepared materials. They reported that a Harshaw3266 supported nickel catalyst altered the gas composition to give a methane rich composition at low temperatures 550-560° C, but the composition was closer to a syngas at high temperatures 740-760° C [68]. Kinoshita et al. [70] performed parametric tests on the catalytic reforming of tars, which are produced during the gasification of biomass using a bench-scale fluid-bed catalytic reformer and a commercial nickel catalyst (United catalyst G-90B 11% nickel on a ceramic support). Minowa et al. [72] investigated two nickel catalysts for the gasification of wood and cellulose at as low as 350° C and 17 MPa in an autoclave. On increasing the catalyst loading, the gas yield increased at the expense of the liquid fraction, and the hydrogen content also increased significantly at this low temperature.

Effect of Temperature

Lugano et al. [80] studied coffee husk gasification using a high temperature air/steam agent. The study findings exhibited the positive influence of high temperature on increasing the gasification process. Furthermore, increased gasification temperature led to a linear increment of CO concentration in the syngas for all gasification conditions. Umeki et al. [81] worked on high temperature steam-only gasification of woody biomass. The tar concentration in the produced gas from the high temperature steam gasification process was higher than that from the oxygen-blown gasification processes. Tremel et al. [82] studied Coal and char properties in high temperature entrained flow gasification at 1200, 1400 and 1600° C. At 1200° C, the intrinsic reactivity of char decreases by a factor of almost 7 from 0.5 s to 2 s residence time, but surface area (approximately 500 m²/g) is hardly affected. At 1400° C and 1600° C, the intrinsic reactivity also decreases, but simultaneously the surface area is reduced to below 300 m²/g. Wu et al. [83] studied the effects of gasification temperature and catalyst ratio on hydrogen production from catalytic steam pyrolysis-gasification of polypropylene. Increasing the gasification temperature resulted in a marked increase in potential hydrogen production from 13.4 to 52.0 wt %, as the gasification temperature was increased from 600 to 900° C. In addition, the CO concentration increased from 9.3 to 27.2 vol %, and CO₂ concentration decreased from 17.8 to 4.5 vol % when increasing the gasification temperature. Cao et al. [84] studied the temperature of the reactor (at both the top and bottom) and reported that an increase in temperature at the top of the

reactor causes less production of tar contents than at the bottom of the reactor. In coal gasification, tar concentration decreases with the increase of temperature due to the cracking and reforming of tars into lighter hydrocarbons [85-89].

On the other hand, upon increasing biomass in coal gasification, tar contents are increased because biomass plays a key role in producing tar [89]. The results from Sjostrom et al. [90] show that during coal gasification, char yield decreases by reducing the amounts of coal and increasing temperature. Lee et al. [91] also report that the increase in both gas velocity and temperature cause an increase in cold gas efficiency. Lapuerta et al. [92] have noted that carbon conversion remains almost constant with the variation of temperature. They explain that with the rise of temperature, volatile matter content increases but residence time decreases. Asadullah et al. [93] have investigated the coal-biomass co-gasification using different catalysts, and they stated that by increasing temperature over Rh/CeO₂/SiO₂ catalysts, carbon conversion seemed to be much higher than that in the presence of other catalysts. Seo et al. [94], and Kim et al. [95, 96] have used different coals (Indonesian Tinto [sub-bituminous], Australian coal, and Shenwha) and found that gas yield increases with the increase in temperature due to pyrolysis, char gasification, steam reforming, and cracking of hydrocarbons.

Recent Progress: Systematic and Numerical Approach

There are two levels of analysis for the gasification: those that are equilibrium-based with no reference to the gasifier geometry, systematic models; and those high fidelity that a couple of the flow equations with the reacting chemical species and complete discretization of the gasifier geometry. Figure 5 shows how one can place these models according to the time it takes for the reactants to completely convert the feedstock into syngas.

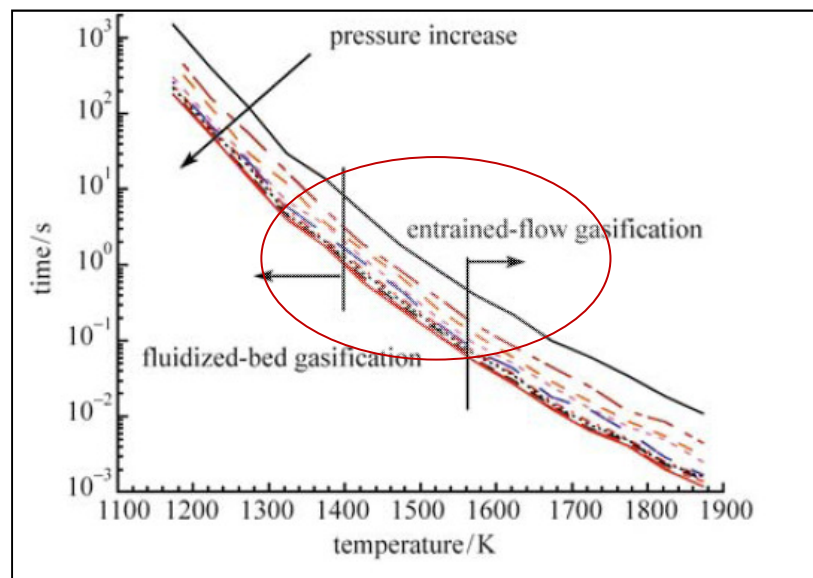


Figure 5. Reaction equilibrium time as a function of pressure and temperature [39]

Gasification in entrained flow gasifiers is amenable to equilibrium, which renders the use of an equilibrium approach. As depicted in Figure 5, the effect of pressures and temperature and the equilibrium time for the homogeneous reactions or the characteristic time scale becomes shorter, indicating that homogenous reactions are fast enough to be considered at equilibrium. For example, an entrained flow reactor operating at high pressure and temperature (1600° K) has an equilibrium time for the syngas homogeneous reaction of less than 0.1s, which is significantly less than the average residence time inside the gasifier. The temperature as depicted, however, has the greatest effect on equilibrium compared to pressure.

Systematic Analysis

There are two main approaches for the developing of a gasification: model equilibrium constant method and the element potential method. The equilibrium constant method can be used to determine the equilibrium species concentrations as well as the temperature and pressure of the products at the gasifier outlet [40]. It is important to realize that this model assumes an infinite residence time, chemical and thermodynamic equilibrium, and hence it neglects the reaction kinetics; nor does it account for the time, mixing or geometry, and hence no spacial distribution of any species. It also has less emphasis on the pollutants as these species govern by slow kinetics and represent the controlling mechanism [10, 26]. These types of models are used to evaluate the gasifier metrics under a best case scenario; i.e., equilibrium and uniform conditions (temperature, heating, pressure, mass flow, etc.). A common list of these reactions is presented in table 4 along with their chemical kinetics.

Table 4. Elementary gasification reaction and their kinetic data

Reaction		Kinetic Parameters A_j , E_j [kJ/mol]
R1	$2 CO + O_2 \rightarrow 2 CO_2$	$A = 10^{17.6}[(m^3mol^{-1})^{-0.75}s^{-1}]$, $E = 166.28 \frac{MJ}{kmol}$
R2	$2 H_2 + O_2 \rightarrow 2 H_2O$	$A = 1e11 [m^3mol^{-1}s^{-1}]$, $E = 42 \frac{MJ}{kmol}$
R3	$CO + H_2O \leftrightarrow CO_2 + H_2$	$A = 0.0265$, $E = 65.8 \frac{MJ}{kmol}$
R4	$C_{(s)} + O_2 \rightarrow CO_2$	$A = 5.67e9 [s^{-1}]$, $E = 160 \frac{MJ}{kmol}$
R5	$C_{(s)} + CO_2 \rightarrow 2 CO$	$A = 7.92e4 [m^3mol^{-1} s^{-1}]$, $E = 218 \frac{MJ}{kmol}$
R6	$C_{(s)} + 2 H_2 \rightarrow CH_4$	$A = 79.2 [m^3mol^{-1} s^{-1}]$ $E = 218 \frac{MJ}{kmol}$

R7	$C_{(s)} + H_2O \rightarrow CO + H_2$	$A = 7.92e4 [m^3mol^{-1} s^{-1}], E = 218 \frac{MJ}{kmol}$
R8	$vol + 0.4 O_2 \rightarrow 1.317 CO$ $+ 2.09 H_2$ $+ 0.064 N_2$	$A = 1E15 [m^3mol^{-1} s^{-1}], E = 1E8 \frac{MJ}{kmol}$

In principle, all the available oxygen in is consumed during the combined heterogeneous and homogeneous reactions gasification reactions [1]. As the oxygen is consumed combustion reactions do not contribute to the equilibrium composition and only the last three reactions are typically considered. In these reactions, a solid carbon feedstock is consumed and the products are limited to CO, CO₂, CH₄, H₂, and H₂O. The objective would be to solve for these five species, oxygen ratio per feedstock, and steam ratio per feedstock for gasification at a certain specified temperature and pressure, thus a total of seven unknowns are generated. Each of above reaction equations is independent, and has an associated equilibrium equation in terms of either the concentration [i] or partial pressure P_i of the species as follows:

$$K_c(T) = \frac{[C]^c [D]^d}{[A]^a [B]^b} \quad \text{or} \quad K_p(T) = \frac{P_C^c \cdot P_D^d}{P_A^a \cdot P_B^b} \quad (2)$$

where $K_c(T) = K_p(T) \cdot (RT)^{c+d-a-b}$

The K_c is the Arrhenius rate and is written as

$$k_c(T) = A_r T^{\beta_r} e^{-\frac{E_r}{RT}} \quad (3)$$

In the above equations, A is the pre-exponent constant, β is temperature exponent constant, E is the activation energy, R is the universal gas constant ($R = 8.313 \text{kJ/kmol} \cdot \text{K}$), and T is the absolute temperature.

The elemental mass conservation for C, H and O add another three equations used to solve the system. An additional equation is the energy equation resulting in a total of seven equations making the problem closed and well defined. The steady form of the energy equation is written as

$$\sum_{i=1}^{n \text{ product}} \dot{n}_i h_i = \sum_{i=1}^{n \text{ reactant}} \dot{n}_i h_i + \dot{Q} \quad (4)$$

The enthalpy terms include enthalpies of formation and sensible enthalpies. The six species, oxygen ratio per feedstock, and steam ratio per feedstock can be solved iteratively. The model can also account for the production of NH₃, H₂S, and COS as traces that are solved for consequently and not in a coupled mode, since the equilibrium model does not account for pollutant formation (no kinetics involved). The feedstock is defined by supplying its proximate and ultimate composition in addition to its lower heating value in the current analysis. Results of coal gasification are depicted in figure 6 from the authors' work and Li et al. [16].

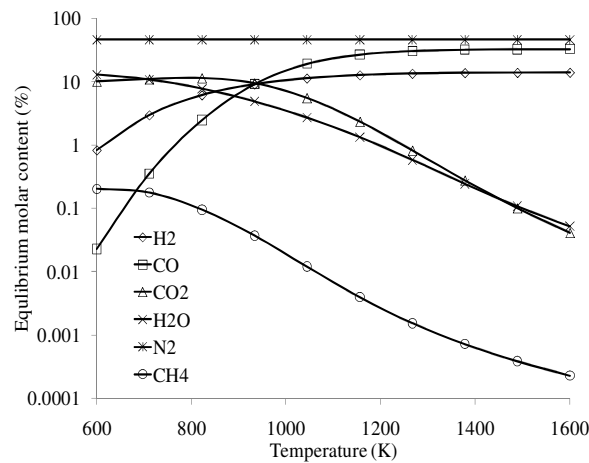
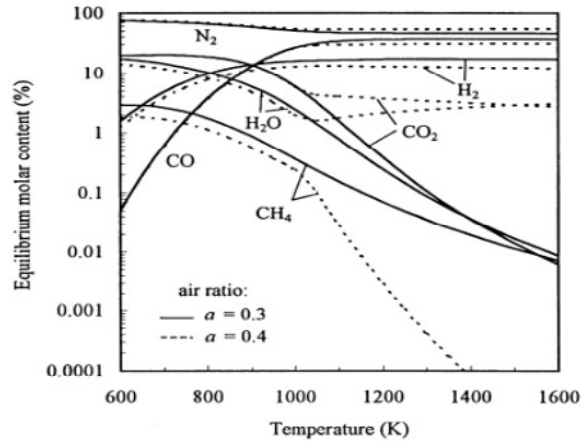


Figure 6. Validation of equilibrium gas composition of high-value coal (top [16], bottom authors' result)

Other work includes Khadse et al. [97], who worked on equilibrium modeling of the gasification of sawdust, bagasse, subabul, and rice husks. The gross calorific value (GCV) variation with temperature suggests that as temperatures increase, GCV increases. At temperatures greater than 1100° K, GCV remains constant for all biomasses. At air 0.1 moles and steam/air=8, all samples give maximum GCV. The GCV of bagasse is the highest and that of subabul is the lowest at lower temperature (<1000° K). At a higher temperature, GCV remains constant. The adiabatic temperature and GCV decrease with an increase in steam/air ratio except for rice husks.

Syed et al. [98] worked on thermodynamics equilibrium analysis within the entrained flow gasifier environment using four different feedstocks. Their result shows that, on a dry and ash-free basis, the maximum gasification efficiency of 68.5%, 76.0%, 76.5% and 74.0% can be achieved for RTC coal, pine needles, plywood, and lignite, respectively. The trend of the results shows that the maximum CGE is achieved when most of the solid carbon present in the feedstock is converted into carbon monoxide. They also show that increasing O/C and

H/C ratio directly affects the CGE. The increase in the value of both ratios gives a raise to the CGE.

Ramanan et al. [99] modeled cashew nut shell char gasification using a chemical equilibrium approach, and their results were validated experimentally. The sensitivity analysis revealed that the mole fraction of H₂, CO, and CH₄ decreases, while CO₂, N₂, and H₂O increases with ER and H₂, CH₄, CO₂, N₂, and H₂O increases, and CO decreases with the moisture content. The HHV of the gas predicted by stoichiometric and nonstoichiometric models was observed to deviate from the experimental results by +17.89 and +1.32%, respectively. Li et al. [100] reported on an equilibrium modeling of gasification using a free energy minimization approach. The model considers five elements and 44 species in both the gas and solid phases. The gas composition and heating values vary primarily with temperature and the relative abundance of key elements, especially carbon, hydrogen and oxygen. Pressure only influences the result significantly over a limited temperature range. The model also predicts the onset of formation of solid carbon, where the gas composition becomes insensitive to additional carbon.

Jarunthammachote and Dutta [104] studied gasification in spouted beds using equilibrium modeling approach. The Gibbs free energy minimization method was used to predict the composition of the producer gas. The major six components, CO, CO₂, CH₄, H₂O, H₂, and N₂ were determined in the mixture of the producer gas. The results showed that the carbon conversion in the gasification process plays an important role in the model. The agreements of the calculated and experimental values of HHV, especially in the case of the circular split spouted bed and the spout-fluid bed, were observed. Vaezi et al. [105] developed a numerical algorithm based on thermochemical equilibrium approach for the simulation of the heavy fuel oil gasification process. Through a parametric study, it was shown that the gasification of heavy fuel oil at a low equivalence ratio of 0.32 makes it possible to obtain a syngas with a considerable calorific value of about 15 MJ/m³. The parametric study also revealed that the gasification pressure had no significant effects on gasification characteristics. The simulations performed in the course of their study suggest that the heavy oil gasification is a feasible process that can be utilized to generate a syngas for various industrial applications.

Karmakar and Datta [101] performed the biomass gasification using rice husks as feedstock. An equilibrium-based model is developed and validated with the experimental results. They used an externally heated gasifier to get the maximum yield of hydrogen in the syngas. Steam is used as the gasifying and oxidizing agent. A parametric study of varying reactor temperature, steam-to-biomass ratio, was also performed to measure the effect on the yield of hydrogen gas. The result shows that the hydrogen contents in the product gas increase with the increase in the reactor temperature and increase in the steam-to-biomass ratio. On other hand, the yield of carbon monoxide increases with the increase in temperature but decreases with increasing steam-to-biomass, ration. Maximum yield of 53% of hydrogen is achieved, while the cold gasification efficiency lies in the range of 63-66%.

Martínez et al. [102] performed the gasification of biomass (eucalyptus wood) using a moving bed downdraft gasifier. A low-fidelity equilibrium model was developed using the mass and energy balance found to be consistent with the experimental results. Air is used as

the gasification agent that is supplied in two different stages to reduce the tar contents and convert biomass into light hydrocarbon. A parametric study was performed by varying the equivalence ratio and by changing the ratio of inlet air in the two stages. The result shows that the maximum coal gasification efficiency of 68% is achieved at the equivalence ratio of 0.4. The yield of syngas at this condition is measured to be 19.04%, 0.89% and 16.78% for CO, CH₄, and H₂, respectively. The results suggest that the considerable reduction in the yield of methane is attributed to the cracking of biomass in the pyrolysis zone by supplying the air in the two stages.

Acharya et al. [104] performed the gasification of biomass (sawdust) in a fixed bed gasifier and has developed a computational model based on Gibbs' free energy minimization. It initially over-predicted the yield of hydrogen gas but adding a corrector equation reduced the error. The gasification is performed in the presence of calcium oxide, while air is used as oxidizer and steam is used as moderator. A parametric study was performed to measure the maximum yield of hydrogen by varying steam to biomass ratio, temperature and CaO/biomass ratio. The experimental result shows that the maximum yield of 54.43% of hydrogen is achieved at CaO/biomass ratio of 2, temperature at 670° C and steam/biomass ratio of 0.83. The effect of including CaO shows that the yield of hydrogen increase from 23.29% (at CaO/biomass=0) to 54% (at CaO/biomass=2). Although an overall efficiency of the process was not calculated, the maximum yield of hydrogen gas shows high gasification efficiency.

Numerical Modeling. The actual gasifier operations suffer from heat losses to the environment, kinetic limitations, turbulence, and dynamic limitations and hence always achieve lower efficiencies than the equilibrium case. Figure 7 illustrates the details of a high fidelity computational scheme. Among all the modeling levels in presented Figure 7 that start by discretizing the gasifier domain via finite grid mesh, the discrete-continuous phases coupling and chemical kinetic reaction deserve further clarification. In applications of gasification and combustion, there exists strong coupling between the Lagrangian (discrete/solid phase) and Eulerian (continuous/gas phase) frames. Therefore, two-way coupling between the discrete phase and the continuous phase is necessary. The gas phase influences the particles via drag, turbulence, and momentum transfer, while the particles influence the gas phase through source terms of mass, momentum, and energy. Examples of coupling include droplet evaporation, devolatilization, and surface combustion as illustrated in Figure 8. The discrete solid particle phase is solved in a Lagrangian frame of reference. This phase consists of spherical particles of 0.1mm diameter dispersed in the continuous phase. Their trajectory is predicted by integrating the force balance on the particle. This force balance equates the particle inertia with the forces acting on the particle and can be described as

$$\frac{d\vec{u}_p}{dt} = F_D (\vec{u} - \vec{u}_p) + \vec{g}(\rho_p - \rho)/\rho_p \quad (5)$$

where $F_D (u - u_p)$ is the drag force per unit particle mass; u is the fluid phase velocity; u_p is the particle velocity; ρ is the fluid density, and ρ_p is the density of the particle. The trajectory equations are solved by stepwise integration over discrete time steps. Integration of equation

5 yields the velocity of the particle at each point along the trajectory, with the trajectory itself predicted according to

$$\frac{dx}{dt} = u_p \quad (6)$$

Equations 5 and 6 are solved for each coordinate direction to predict the trajectories of the discrete phase. The trajectories of the discrete phase particles are computed as well as their heat and mass transfer. Stepwise conversion laws are applied to these solid particles, starting with inert heating law, as the particle temperature is below the vaporization temperature followed with demoiaturization/evaporation law for the release of moisture, then devolatilization law, and finally combustion law. For example, the devolatilization law is applied to the combusting particle mass (m_p) when the temperature of the particle reaches the specified devolatilization temperature, at which the mass evolution continues and is written as

$$-\frac{dm_p}{dt} = Ae^{-(E/RT)} [m_p - (1 - f_v^0)m_p^0] \quad (7)$$

where f_v , and m_p^0 are the volatile fraction and initial mass, respectively. It remains in effect while the mass of the particle, m_p , exceeds the mass of the non-volatiles in the particle. The heat transfer to the particle during devolatilization process governs the contributions from convection, radiation, and the heat consumed during devolatilization and is written as

$$m_p c_p \frac{dT_p}{dt} = hA_p(T_\infty - T_p) + \frac{dm_p}{dt} h_{fg} + \epsilon_p A_p \sigma (T_R^4 - T_p^4) \quad (8)$$

where c_p , h_{fg} , A , and σ are specific heat, latent heat of evaporation, particle surface area, and Stefan constant, respectively. After the volatile component of the particle is completely evolved, a surface reaction begins, which consumes the combustible fraction of the particle until the combustible fraction is consumed. Heat, momentum, and mass transfer between the solid fuel particles and the gas will be included by alternately computing the discrete phase trajectories and the continuous phase equations.

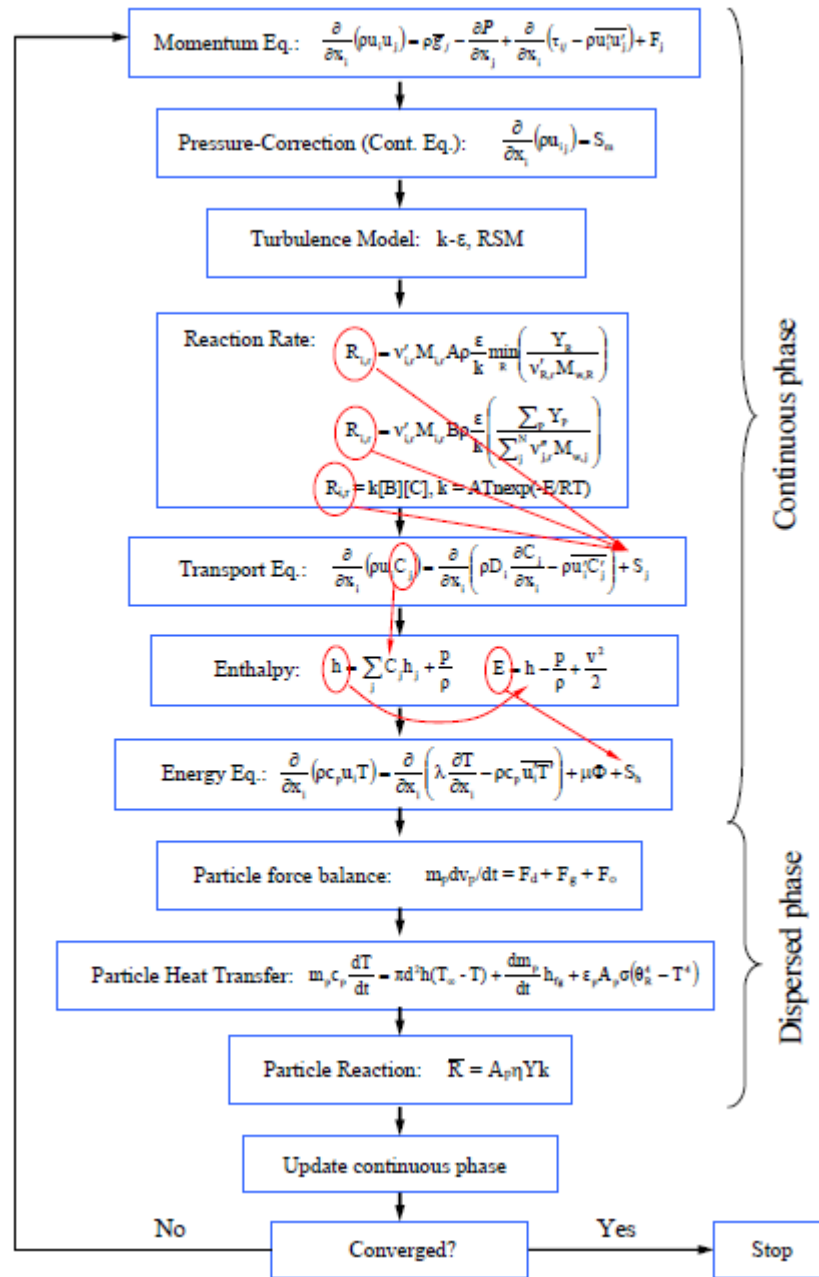


Figure 7. Numerical scheme outline [50]

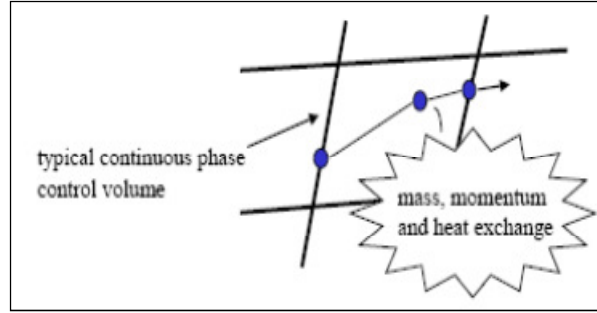


Figure 8. Coupling between discrete and continuous phase in Lagrangian-Eulerian frame where exchange of mass, momentum, and heat between the discrete and continuous phases within a control volume crossed by the particle.

The reactions are modeled using the species transport model and both volumetric and surface reactions are included. The turbulence-chemistry interaction is modeled using the finite-rate/eddy-dissipation option. The net rate of production of species i (R_i), which presents, as a source (Si) in the transport equation, is determined based on the minimum of both the Arrhenius and the eddy-dissipation reaction rates:

$$R_{i,r} = \dot{v}_{i,r} M_{i,r} A \rho \frac{\varepsilon}{k} \min \left(\frac{Y_R}{\dot{v}_{R,r} M_{w,R}} \right) \quad (9)$$

$$R_{i,r} = \dot{v}_{i,r} M_{i,r} B \rho \frac{\varepsilon}{k} \left(\frac{\sum p Y_P}{\sum_j^N v''_{j,r} M_{w,j}} \right) \quad (10)$$

where $\dot{v}_{i,r}$ is the stoichiometric coefficient of reactant i in reaction r and $v''_{j,r}$ is stoichiometric coefficient of product j in reaction r . Y_R and Y_P are the mass fraction of reactant R and product P respectively. A and B are tunable empirical constants and k and ε are the turbulence kinetic energy and its dissipation rate. When the remaining devolatilized solid char particle and the oxidizer react, they form either CO or CO₂; therefore, an additional heterogeneous (or surface) reaction for the discrete particles is required and is typically written as

$$\bar{R}_{i,r} = A \eta_r Y_r R_{i,r} \text{ with } R_{i,r} = K_{kin,rc} \left[p_j - R_{i,r} / D_{o,r} \right]^{N_r} \quad (11)$$

where A is the particle surface area, η is the effective factor, Y_i is the mass fraction of species i , R is the rate of reaction, K here is the kinetic rate of reaction, and p is the bulk partial pressure of the species i , D is the diffusion rate coefficient for reaction r and N_r is apparent order of the reaction r . Authors' results of a typical high-fidelity model are depicted in Figure 9.

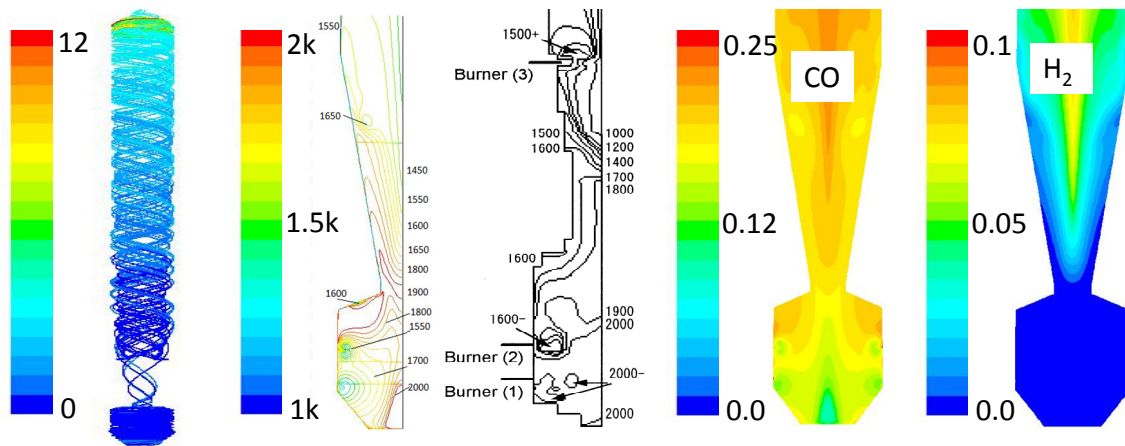


Figure 9. Trajectory of the flow colored by residence time, temperature distribution compared to Chen et al., and CO and H₂ molar fraction distribution of the authors' mode.

Chen et al. [106] investigated the performance of a two-stage, entrained-flow gasifier upon scale up and emphasized the effect of the burner diameter on the swirl flow, and hence on the build-up of ash/slag on the gasifier walls. They recommended having a smaller diameter for the combustion zone burner followed by a slightly larger (intermediate) diameter for the redactor burner. Bockelie et al. [107] developed a CFD code using Glacier, an updated tool that is well known for its strong coupling between the different physical processes occurring in a gasification environment, for entrained flow gasifiers of two types that are commercially dominant: the down-fired GE gasifiers with one stage and two-stage, updraft gasifier with multiple inlets. Equilibrium was assumed for all the chemical reactions and an Eulerian-Lagrangian approach was followed. The effect of various devolatilization models was studied and a slagging model was suggested to comprehensively model the gasifier since the flow of hot mineral fluid on gasifier walls is crucial to realistically predict the gasifier performance.

Watanabe and Otaka [108] developed a three-dimensional model for a 2-ton per day research scale coal entrained flow gasifier. The effect of air ratio on gasification performance, such as char conversion, syngas composition, and cold-gas efficiency was studied. The model predicted results were in reasonable agreement with experimental data. The study concluded that increasing the air ratio increases carbon conversion; however, it decreases the heating value of the syngas due to the excess oxidative effect of air on the syngas. Shi et al., [105] modeled a slurry, two-stage, oxygen-blown, entrained flow, coal gasifier following an Eulerian-Lagrangian approach. The model syngas composition was found to be in agreement with an equilibrium reactor model that represents experimental data (using Aspen Plus). Aspen Plus was used only to “globally” check the validity of the CFD model, since Aspen Plus follows a reduced order methodology.

Fletcher et al. [109] developed a comprehensive model using CFX 4 to simulate an entrained flow biomass gasifier. Particles were tracked using a Lagrangian approach. Emphasis was given to the devolatilization model, which predicts the composition of the volatiles by knowledge of elemental composition and fixed carbon content of the biomass and assuming the heat of combustion of the volatiles is equal to the higher heating value of the biomass.

Volatile composition was found for sawdust and cotton trash. Fletcher et al. [25] found that the significant changes in the gas density and flow rate as a result of the reactions (combustion and gasification) cause the flow to become less affected by the turbulence and hence the less expensive model (k- ϵ) was selected. The producer gas for cotton trash was found to have 11% CO and 23% H₂ by volume. Kumar [111] worked on a multi-scale CFD simulation of entrained flow gasification. Higher operating pressure led to higher carbon conversion, and increasing the gasifier mass throughput reduced carbon conversion. The residence time, average particle temperature during conversion, and pressure effect on kinetics are the key factors that influence the overall carbon conversion when the operating pressure and gasifier mass throughput are varied.

Hampp and Janajreh [112] carried out the development of a drop tube reactor (DTR) using CFD analysis to get optimal conditions of the velocity, temperature, and residence time while varying the mass flow rate and heat flux. The results showed that the velocity depends more on the MFR while the temperature is more predictable with the HF. Talab et al. [113] also investigated numerical modeling of coal/tire-shred co-gasification using 5, 10 and 20% tire in coal, using an entrained flow gasifier, and observed an increase in the particle burn out rate with high tire composition in the mixture. Janajreh et al. [114] studied numerical modeling of flow in an entrained flow gasifier using coal only and observed results comparable with experimental values.

Janajreh and Al-Shrah [115] investigated the downdraft gasification of wood chips numerically and experimentally. A commercial downdraft gasifier scaled for 10–20 kW batched with wood chips of medium size (0.5 cm thickness, 1–2 cm width, and 2–2.5 cm length) was operated, and the temperatures at ten different locations along gasifier were recorded. It was shown that the density in terms of the heating value and moisture content of the feedstock significantly affected reactivity. The consumption of the batch of wood was relatively fast, in the order 25 minutes, suggesting the importance of using a higher fixed carbon content (dense) feedstock or continuous feeding rather than semi-batched. The average temperature computed by CFD was higher compared to that measured experimentally and comparable to the calculated ideal one, which corresponds to equilibrium conditions.

Sun et al. [116] developed a comprehensive three-dimensional model to simulate a coal water slurry entrained flow gasifier. The model is divided into several sub models that included water evaporation, coal pyrolysis, heterogeneous, and homogeneous reaction. Rosin-Rammler distribution was used for the particle size distribution, while water evaporation rate is modeled by bulk steam partial pressure and steam saturation pressure at the surface. Coal devolatilization was modeled by using the Kobayashi model. Five different homogeneous reaction are included in the simulation using the Arrhenius-based reaction rate and the turbulent mixing rate by taking the minimum of these two. For modeling the heterogeneous reaction, an experiment was performed using the DTR to measure the conversion rate of char. After the building of computational model, it was validated using the industrial operated data from the gasifier in terms of syngas yield, carbon conversion, and temperature. The results show that the model accurately calculated the yield of syngas within a few percentage errors, while carbon conversion was accurately calculated and the temperature

difference was only 10° C overestimated. Further flow field, temperature, and composition distribution inside the gasifier was studied, as well as the effect of oxygen/coal ratio and slurry concentration on the performance of gasifier. The results show that the increase in oxygen/coal ration decreased the cold gas efficiency, and high slurry concentration led to high temperature and high cold gas efficiency, with slight decreases in carbon conversion. Luan et. al. [117] simulated a three-dimensional, steady state, Navier-Stokes based model to analyze the performance of a pressurized oxygen-blown entrain flow gasifier.

ANSYS/Fluent was used to simulate the gasifier by treating coal particle as a discrete phase and model via discrete phase model. The turbulence was modeled by using a standard k-ε model, radiation was modelled using a P1 radiation model, and species transport equations were solved by using finite rate/eddy dissipation model. A total of eight global reactions were used in which three reactions defined the char conversion. Arrhenius-based reaction rates were used to define the reaction. Furthermore, the model was run to analyze the effect of oxygen/coal ratio, coal slurry concentration, and the effect of first and second stage fuel distribution. The results showed that the increase in oxygen/coal ratio led to higher exit temperature, with higher carbon dioxide and lower carbon monoxide that eventually led to lower the cold gasification efficiency. The increase in coal slurry showed the reduction of hydrogen, carbon dioxide, and water, while the increase in the quantity of carbon monoxide was calculated. Their comparative study for first and second stage fuel feeding suggested that the 78% and 22% of coal slurry injection give a marginally higher syngas heating value and cold gasification efficiency.

Xie et al. [118] developed a three-dimensional numerical model to simulate the gasification of solid waste, beech wood. The gas phase was modelled using the large eddy simulation turbulent model. while particle phase was modeled by the Lagrangian method. Thirteen global reactions were used to model both homogeneous and heterogeneous phases of the gasification. Air and steam were used as the oxidization agents at atmospheric pressure. Finally, the effect of the equivalence ratio was investigated on the yield of the syngas. The result showed that an increase in the equivalence ratio from 0.20-0.24 decreased the yield of hydrogen and carbon monoxide in the product syngas. The mole fraction of hydrogen and methane was more than the experimental value, which is due to ignoring tar and light hydrocarbon in the model. The temperature distribution ranged from 750° K to 900° K inside the gasifier.

Conclusions

Undoubtedly, gasification reactions are complex, and detailed analysis is necessary for reliable predictions. It all starts with an accurate feedstock characterization of the amount of moisture, volatile, fixed carbon, and the inorganics that provides a unit feedstock formula. A lump sum systematic approach that lacks the inclusion of detailed devolatilization model, global homogenous and heterogonous reaction mechanisms, and tar formation mechanism has lesser value. Actual operating gasifiers, such as Texaco, Shell, and GE, have reported the existence of tars even at high temperatures exceeding 1000° C [19] that add more complexity for any level of modeling. Material characterization is a critical step in modeling gasification processes, since information about the feedstock heating value and composition are necessary

to predict its empirical formula and hence its reactions' stoichiometry. Predicting the empirical formula of volatiles is essential to achieve the volatiles' breakup equation mass balance. Entrained flow gasifiers are amenable to equilibrium modeling. Equilibrium-based model are idealistic (infinite reaction time and neither has kinetic nor mass transfer limitation), and their results at the gasifier exit exhibit large deviations from the detailed CFD computations. Previous research [10] has shown that concentrations close to equilibrium values can be achieved in quasi-equilibrium environments (where kinetic limitations exist) at higher temperatures in the range of 200° more than the corresponding temperature in an equilibrium environment.

Although CFD is a powerful tool in simulating fluid flow, complex scenarios such as turbulence and solid surface reactions are still challenging. Therefore, it is very important to validate any results against experimental data. However, there exists a scarcity in available experimental data, especially when compared to the limitless discrete data computed by CFD. The reliability of any model depends, among other things, on the accuracy of kinetic data for the chemical reactions including the important initial step of devolatilization. The authors' work incorporates an experimentally-based devolatilization scheme in their simulations that was found to compare better with experimental data than the proposed computed results of Chen et al. [106].

Acknowledgment

The support of Masdar Institute and the Waste to Energy Laboratory group is highly appreciated.

References

- [1] Harris, E. (2002). *Climate Change Action Plan*. Aberdeen, Scotland: Aberdeen City Council.
- [2] Thompson, L. G., Brecher, H. H., Mosley-Thompson, E., Hardy, D. R., & Marka, B. G. (2009). Glacier Loss on Kilimanjaro Continues Unabated. *Proceedings of the National Academy of Sciences*. Retrieved from <http://www.pnas.org/content/early/2009/10/30/0906029106.full.pdf+html>
- [3] Prins, M. J., Ptasiński, K. J. & Jansen, F. J. J. G. (2007). From Particle to Biomass Gasification: Comparison of Thermodynamic Efficiency. *Energy*, 32(7), 1248-1259.
- [4] Raveendran, K., Ganesh, A., & Khilar K. C. (1995). Influence of Mineral Matter on Biomass Pyrolysis Characteristics. *Fuel*, 74(12), 1812-22.
- [5] Talab, I. (2011). *Carbonaceous Material Gasification: Zero-Dimensional Analysis and Development of Computational Fluid Dynamics Model for an Entrained Flow Gasifier*. (Master's thesis). Masdar Institute.
- [6] Higman, C., & Van der Burgt, M. (2003). *Gasification*. Houston: Gulf Professional Publishing.
- [7] Dasappa, S., Paul, P. J., Mukunda, H. S., Rajan, N. K. S., Sridhar, G., & Sridhar, H. V. (2004). Biomass Gasification Technology—A Route to Meet Energy Needs, *Current Science*, 87(7), 908-916.

- [8] Balat, M., Balat, M., Kırtay, E., & Balat, H. (2009). Main Routes for the Thermo-Conversion of Biomass into Fuels and Chemicals: Part 2: Gasification Systems. *Energy Conversion and Management*, 50(12), 3158-3168.
- [9] McKendry, P. (2002). Energy Production from Biomass (Part 1): Overview of Biomass. *Bioresource Technologies*, 83(1), 37-46.
- [10] McKendry, P. (2002). Energy Production from Biomass (Part 3): Gasification Technologies. *Bioresource Technology*, 83(1), 55-63.
- [11] Li, X. (2002). *Biomass Gasification in Circulating Fluidized Bed*. (Doctoral dissertation), University of British Columbia.
- [12] Kishore, V. V. N. (ed.). (2008). *Renewable Energy Engineering & Technology: A Knowledge Compendium*. New Delhi: TERI Press.
- [13] Rauch, R. (2003). *Thermal Gasification of Biomass, IEA Bioenergy Agreement, Task 33*. Retrieved from <http://www.ieabioenergy.com/task/thermal-gasification-of-biomass/>
- [14] Carlos L. (2005). *High Temperature Air/Steam Gasification of Biomass in an Updraft Fixed Bed Type Gasifier*. (Doctoral dissertation), Royal Institute of Technology, Stockholm.
- [15] Reed T. B., & Das, A. (1988). *Handbook of Biomass Downdraft Gasifier Engine Systems*. Golden, CO: Solar Energy Research Institute.
- [16] Knoef H. A. M. (2005). *Handbook of Biomass Gasification*. Meppel, The Netherlands: BTG Biomass Technology Group B.V.
- [17] E4tech. (2009). Review of Technologies for Gasification of Biomass and Wastes. NNFCC Project 09/008. Retrieved from <http://wiki.gekgasifier.com/f/Review+of+Biomass+Gasification+Technologies.NNFCC.Jun09.pdf>
- [18] Phillips, J. (2006). Different Types of Gasifiers and Their Integration with Gas Turbines. In NETL (Ed.), *The Gas Turbine Handbook*. Retrieved from <http://www.netl.doe.gov/research/coal/energy-systems/turbines/reference-shelf/handbook>
- [19] Olafsson, I., Nordin, A. & Söderlind, U. (2005). *Initial Review and Evaluation of Process Technologies and Systems Suitable for Cost-Efficient Medium-Scale Gasification for Biomass to Liquid Fuels*. ETPC report 05:02. Umeå: Umeå University.
- [20] Ciferno, J. P. & Marano, J. J. (2002). *Benchmarking Biomass Gasification Technologies for Fuels, Chemicals and Hydrogen Production*. Retrieved from <http://www.netl.doe.gov/File%20library/research/coal/energy%20systems/gasification/BMassGasFinal.pdf>
- [21] Ising, M., Unger, C., Heinz, A., & Althaus, W. (2002). Cogeneration from Biomass Gasification by Producer Gas-Driven Block Heat and Power Plants. *Proceedings of the 12th European Biomass Conference*, Amsterdam, 1033-1036.
- [22] Hofbauer, H. (2006). *Gas-Cleaning at the Güssing Plant, Update*. ThermalNet: Intelligent Energy Europe.
- [23] Hofbauer, H., Rauch, R., Bosch, K., Aichernig, C. & Koch, R. (2007). *Biomass CHP-Plant Güssing: A Success Story*. Vienna: University of Technology.

- [24] Rauch, R. (2006). Fluidised Bed Gasification and Synthetic Biofuels, the Güssing Plant. *Proceedings of the European Conference on Biorefinery Research*, Helsinki. Retrieved from http://ec.europa.eu/research/energy/pdf/gp/gp_events/biorefinery/bs3_03_rauch_en.pdf
- [25] Paisley, M. A. & Overend, R. P. (2002). Verification of the Performance of Future Energy Resources' SilvaGas Biomass Gasifier—Operating Experience in the Vermont Gasifier. *Proceedings of the Pittsburgh Coal Conference*, Pittsburgh.
- [26] Paisley, M. A. & Welch, M. J. (2003). Biomass Gasification Combined Cycle Opportunities Using the Future Energy Silvagasgasifier Coupled to Alstom's Industrial Gas Turbines. *Proceedings of ASME Turbo Expo*, Atlanta.
- [27] Dinjus, P., Dahmen, N., & Koerber, R. (2008). Synthetic Fuel from Biomass—The Bioliqour Process. *IFAT Proceedings, 3rd International Trade Fair for Water, Sewage, Refuse, Recycling and Natural Energy Sources*, Shanghai.
- [28] Henrich, E. (2007). *The Status of the FZK Concept of Biomass Gasification*. (2nd ed.). European Summer School on Renewable Motor Fuels, Warsaw. Retrieved from <http://www.baumgroup.de/Renew/download/5%20-%20Henrich%20-%20paper.pdf>
- [29] Advanced Plasma Power. (2007). *Gasplasma Outputs—Clean Syngas: The Effects of Plasma Treatment on the Reduction of Organic Species in the Syn-Gas*.
- [30] Patel, J. (2004). Biomass Gasification Gas Engine Demonstration Project. *Conference on Small Wood, Creating Solutions for Using Small Trees*, Sacramento.
- [31] Roberts, D. G., Harris, D. J., & Wall, T. F. (2003). Effects of High Pressure and Heating Rate during Coal Pyrolysis on Char Gasification Reactivity. *Energy Fuels*, 17(4), 887-895.
- [32] Young, C. M. (2006). *Pressure Effects on Black Liquor Gasification*. (Doctoral dissertation), Georgia Institute of Technology.
- [33] Tülay, G. M., Mehmet, S., Mithat, Y., & Levent, B. (2013). Simultaneous Effect of Temperature and Pressure on Catalytic Hydrothermal Gasification of Glucose. *The Journal of Supercritical Fluids*, 73, 151-160.
- [34] Sharma, S., Saito, I., & Takanohashi, T. (2009). Effect of Steam Partial Pressure on Gasification Rate and Gas Composition of Product Gas from Catalytic Steam Gasification of Hypercoal. *Energy and Fuels*. doi: 10.1021/ef900461w
- [35] Malekshahian, M. (2012). *Effect of Pressure on Gasification of Petroleum Coke with Carbon Dioxide*. (Doctoral dissertation), University of Calgary.
- [36] Wall, T. F., Liu, G., Wu, H., Roberts, D. G., Benfell, K. E., Gupta, S., John, A. L. & David, J. H. (2002). The Effects of Pressure on Coal Reactions during Pulverised Coal Combustion and Gasification. *Progress in Energy and Combustion Science*, 28(5), 405-433.
- [37] Cetin, E., Gupta, R., & Moghtaderi, B. (2005). Effect of Pyrolysis Pressure and Heating Rate on Radiata Pine Char Structure and Apparent Gasification Reactivity. *Fuel*, 84(10), 1328-1334.
- [38] Zhang, L. & Calo, J. M. (1996). The Effect of CO₂, Partial Pressure on Gasification Reactivity. *American Chemical Society, Division of Fuel Chemistry*, 41(1), 138-142.
- [39] Sutton, D., Kelleher, B., & Ross, J. R. H. (2001). Review of Literature on Catalysts for Biomass Gasification. *Fuel Processing Technology*, 73, 155-173.

- [40] Orío, A., Corella, J., & Narváez, I. (1997). Characterization and Activity of Different Dolomites for Hot Gas Cleaning in Biomass Gasification. In A. V. Bridgwater & D. G. B. Boocock (Eds.), *Developments in Thermochemical Biomass Conversion* (1144-1157). Amsterdam: Springer.
- [41] Delgado, J., Aznar, M. P., & Corella, J. (1997). Biomass Gasification with Steam in Fluidized Bed: Effectiveness of CaO, MgO, and CaO–MgO for Hot Raw Gas Cleaning. *Industrial & Engineering Chemistry Research*, 36(5), 1535-1543. doi: 10.1021/ie960273w
- [42] Vassilatos, V., Taralas, G., Sjöström, K., & Björnbom, E. (1992). Catalytic Cracking of Tar in Biomass Pyrolysis Gas in the Presence of Calcined Dolomite. *The Canadian Journal of Chemical Engineering*, 70(5), 1008-1013. doi: 10.1002/cjce.5450700524
- [43] Pérez, P., Aznar, P. M., Caballero, M. A., Gil, J., Martín, J. A., & Corella, J. (1997). Hot Gas Cleaning and Upgrading with a Calcined Dolomite Located Downstream a Biomass Fluidized Bed Gasifier Operating with Steam–Oxygen Mixtures. *Energy & Fuels*, 11(6), 1194-1203. doi: 10.1021/ef970046m
- [44] Corella J., Herguido J., Gonzales-Saiz J., Trujillo J. (1988). Fluidized Bed Steam Gasification of Biomass with Dolomite and with a Commercial FCC Catalyst. In A. V. Bridgwater, J .L. Kuester (eds.). *Research In Thermochemical Biomass Conversion*. London: Elsevier.
- [45] Narváez, I., Orío, A., Aznar, M. P., & Corella, J. (1996). Biomass Gasification with Air in an Atmospheric Bubbling Fluidized Bed. Effect of Six Operational Variables on the Quality of the Produced Raw Gas. *Industrial & Engineering Chemistry Research*, 35(7), 2110-2120. doi: 10.1021/ie9507540
- [46] Myrén, C., Hörnell, C., Sjöström, K., Yu, Q., Brage, C., & Björnbom, E. (1997). Catalytic Upgrading of the Crude Gasification Product Gas. In A. V. Bridgwater & D. G. B. Boocock (eds.). *Developments in Thermochemical Biomass Conversion* (1170-1178). Amsterdam: Springer.
- [47] Vassilatos, V., Taralas, G., Sjöström, K., & Björnbom, E. (1992). Catalytic Cracking of Tar in Biomass Pyrolysis Gas in the Presence of Calcined Dolomite. *The Canadian Journal of Chemical Engineering*, 70(5), 1008-1013. doi: 10.1002/cjce.5450700524
- [48] Aldén, H., Björkman, E., Carlsson, M., & Waldheim, L. (1993). Catalytic Cracking of Naphthalene on Dolomite. In A. V. Bridgwater (ed.). *Advances in Thermochemical Biomass Conversion* (216-232). Amsterdam: Springer.
- [49] Simell, P. A., Hakala, N. A. K., Haario, H. E., & Krause, A. O. I. (1997). Catalytic Decomposition of Gasification Gas Tar with Benzene as the Model Compound. *Industrial & Engineering Chemistry Research*, 36(1), 42-51. doi: 10.1021/ie960323x
- [50] Taralas, G., Sjöström, K., & Björnbom, E. (1993). Dolomite Catalysed Cracking of n-Heptane in Presence of Steam. In A. V. Bridgwater (ed.). *Advances in Thermochemical Biomass Conversion* (233-245). Amsterdam: Springer.
- [51] Alden, H., Hagstrom, P., Hallgren, A., & Waldheim, L. (1996). Review of Literature on Catalysts for Biomass Conversion. *Proceedings of Conference on Developments in Thermochemical Biomass Conversion*, Banff, Canada, 1131.
- [52] Simell, P. A., Hepola, J. O., & Krause, A. (1997). Effects of Gasification Gas Components on Tar and Ammonia Decomposition over Hot Gas Cleanup Catalysts, *Fuel*, 76, 117-127.

- [53] Aznar, M. P., Corella, J., Gil, J., Martín, J. A., Caballero, M. A., Olivares, A., . . . Francés, E. (1997). Biomass Gasification with Steam and Oxygen Mixtures at Pilot Scale and with Catalytic Gas Upgrading. Part I: Performance of the Gasifier. In A. V. Bridgwater & D. G. B. Boocock (eds.). *Developments in Thermochemical Biomass Conversion* (1194-1208). Amsterdam: Springer.
- [54] Lammers, G., Beenackers, A. A. C. M., & Corella, J. (1997). Catalytic Tar Removal from Biomass Producer Gas with Secondary Air. In A. V. Bridgwater & D. G. B. Boocock (eds.). *Developments in Thermochemical Biomass Conversion* (1179-1193). Amsterdam: Springer.
- [55] Ekstrom C., Lindman N., Pettersson R., (1996). Catalytic Conversion of Tars, Carbon Black and Methane from Pyrolysis/Gasification of Biomass. *Proceedings of Conference on Developments in Thermochemical Biomass Conversion*, Banff, Canada, 601.
- [56] Mudge, L. K., Baker, E. G., Mitchell, D. H., & Brown, M. D. (1985). Catalytic Steam Gasification of Biomass for Methanol and Methane Production. *Journal of Solar Energy Engineering*, 107(1), 88-92. doi: 10.1115/1.3267660
- [57] Hauserman, W. B. (1994). High-Yield Hydrogen Production by Catalytic Gasification of Coal or Biomass. *International Journal of Hydrogen Energy*, 19(5), 413-419. doi: [http://dx.doi.org/10.1016/0360-3199\(94\)90017-5](http://dx.doi.org/10.1016/0360-3199(94)90017-5)
- [58] Hallen, R. T., Sealock, L. J., Jr., & Cuello, R. (1985). Influence of Alkali Carbonates on Biomass Volatilization. In R. P. Overend, T. A. Milne & L. K. Mudge (eds.). *Fundamentals of Thermochemical Biomass Conversion* (157-166). Amsterdam: Springer.
- [59] Encinar, J. M., Beltrán, F. J., Ramiro, A., & González, J. F. (1998). Pyrolysis/Gasification of Agricultural Residues by Carbon Dioxide in the Presence of Different Additives: Influence of Variables. *Fuel Processing Technology*, 55(3), 219-233. doi: [http://dx.doi.org/10.1016/S0378-3820\(98\)00052-6](http://dx.doi.org/10.1016/S0378-3820(98)00052-6)
- [60] Sada, E., Kumazawa, H., & Kudsy, M. (1992). Pyrolysis of Lignins in Molten Salt Media. *Industrial & Engineering Chemistry Research*, 31(2), 612-616. doi: 10.1021/ie00002a025
- [61] Li, T.-C., Yan, Y.-j., & Ren, Z.-w. (1996). Study on Gasification of Peat and Its Kinetic Behavior. *Fuel Science and Technology International*, 14(7), 879-896. doi: 10.1080/08843759608947618
- [62] DeGroot W.F., Shafizaceh F., (1996), Kinetics of Wood Gasification by carbon Dioxide and Steam. *Proceedings of Conference on Developments in Thermochemical Biomass Conversion*, Banff, Canada, 275.
- [63] Anthony, D. B., & Howard, J. B. (1976). Coal Devolatilization and Hydrogasification. *AIChE Journal*, 22(4), 625-656. doi: 10.1002/aic.690220403
- [64] Gebhard, S. C., Wang, D., Overend, R. P., & Paisley, M. A. (1994). Catalytic Conditioning of Synthesis Gas Produced by Biomass Gasification. *Biomass and Bioenergy*, 7(1-6), 307-313. doi: [http://dx.doi.org/10.1016/0961-9534\(94\)00073-3](http://dx.doi.org/10.1016/0961-9534(94)00073-3)
- [65] Rostrupnielsen, J. R., & Hansen, J. H. B. (1993). CO₂-Reforming of Methane over Transition Metals. *Journal of Catalysis*, 144(1), 38-49. doi: <http://dx.doi.org/10.1006/jcat.1993.1312>

- [66] Aznar, M. P., Caballero, M. A., Gil, J., Martín, J. A., & Corella, J. (1998). Commercial Steam Reforming Catalysts To Improve Biomass Gasification with Steam–Oxygen Mixtures. 2. Catalytic Tar Removal. *Industrial & Engineering Chemistry Research*, 37(7), 2668-2680. doi: 10.1021/ie9706727
- [67] Baker, E. G., Mudge, L. K., & Brown, M. D. (1987). Steam Gasification of Biomass with Nickel Secondary Catalysts. *Industrial & Engineering Chemistry Research*, 26(7), 1335-1339. doi: 10.1021/ie00067a012
- [68] Baker E.G., Mudge L.K., Wilcox W.A., (1996), Catalysis of Gas-Phase Reaction in Steam Gasification of Biomass. *Proceedings of Conference on Developments in Thermochemical Biomass Conversion*, Banff, Canada, 863.
- [69] Elliott, D. C., Baker, E. G., Butner, R. S., & Sealock, J. L. J. (1993). Bench-Scale Reactor Tests of Low Temperature, Catalytic Gasification of Wet Industrial Wastes. *Journal of Solar Energy Engineering*, 115(1), 52-56. doi: 10.1115/1.2930024
- [70] Kinoshita, C. M., Wang, Y., & Zhou, J. (1995). Effect of Reformer Conditions on Catalytic Reforming of Biomass-Gasification Tars. *Industrial & Engineering Chemistry Research*, 34(9), 2949-2954. doi: 10.1021/ie00048a004
- [71] Roy, C., Pakdel, H., Zhang, H. G., & Elliott, D. C. (1994). Characterization and Catalytic Gasification of the Aqueous By-Product from Vacuum Pyrolysis of Biomass. *The Canadian Journal of Chemical Engineering*, 72(1), 98-105. doi: 10.1002/cjce.5450720115
- [72] Minowa, T., Ogi, T., Dote, Y., & Yokoyama, S.-y. (1994). Methane Production from Cellulose by Catalytic Gasification. *Renewable Energy*, 5(5-8), 813-815. doi: [http://dx.doi.org/10.1016/0960-1481\(94\)90094-9](http://dx.doi.org/10.1016/0960-1481(94)90094-9)
- [73] Wang, D., Czernik, S., & Chornet, E. (1998). Production of Hydrogen from Biomass by Catalytic Steam Reforming of Fast Pyrolysis Oils. *Energy & Fuels*, 12(1), 19-24. doi: 10.1021/ef970102j
- [74] Sánchez, J. L., García, L., Salvador, M. L., Bilbao, R., Arauzo, J., & Fang, Z. (1997). Black Liquor Pyrolysis and Char Reactivity. In A. V. Bridgwater & D. G. B. Boocock (eds.). *Developments in Thermochemical Biomass Conversion* (294-304). Amsterdam: Springer.
- [75] Garcia, L., Salvador, M. L., Arauzo, J., & Bilbao, R. (1998). Influence of Catalyst Weight/Biomass Flow Rate Ratio on Gas Production in the Catalytic Pyrolysis of Pine Sawdust at Low Temperatures. *Industrial & Engineering Chemistry Research*, 37(10), 3812-3819. doi: 10.1021/ie9801960
- [76] Yamaguchi, T., Yamasaki, K., Yoshida, O., Kanai, Y., Ueno, A., & Kotera, Y. (1986). Deactivation and Regeneration of Catalyst for Steam Gasification of Wood to Methanol Synthesis Gas. *Industrial & Engineering Chemistry Product Research and Development*, 25(2), 239-243. doi: 10.1021/i300022a019
- [77] Arauzo, J., Radlein, D., Piskorz, J., & Scott, D. S. (1997). Catalytic Pyrogasification of Biomass. Evaluation of Modified Nickel Catalysts. *Industrial & Engineering Chemistry Research*, 36(1), 67-75. doi: 10.1021/ie950271w
- [78] Richardson, S. M., & Gray, M. R. (1997). Enhancement of Residue Hydroprocessing Catalysts by Doping with Alkali Metals. *Energy & Fuels*, 11(6), 1119-1126. doi: 10.1021/ef9700011

- [79] Bangala, D. N., Abatzoglou, N., & Chornet, E. (1998). Steam Reforming of Naphthalene on Ni–Cr/Al₂O₃ Catalysts Doped with MgO, TiO₂, and La₂O₃. *AIChE Journal*, 44(4), 927-936. doi: 10.1002/aic.690440418
- [80] Wilson, L., John, G. R., Mhilu, C. F., Yang, W., Blasiak, W. (2010). Coffee Husks Gasification Using High Temperature Air/Steam Agent. *Fuel Processing Technology*, 91(10), 1330-1337.
- [81] Yamamoto, K., Namioka, T., & Yoshikawa, K. (2010). High Temperature Steam-Only Gasification of Woody Biomass. *Applied Energy*, 87(3), 791-798.
- [82] Tremel, A., Haselsteiner, T., Nakonz, M., & Spliethoff, H. (2012). Coal and Char Properties in High Temperature Entrained Flow Gasification. *Energy*, 45(1), 176.
- [83] Wu, C., & Williams, P. T. (2008, November). Effects of Gasification Temperature and Catalyst Ratio on Hydrogen Production from Catalytic Steam Pyrolysis-Gasification of Polypropylene. *Energy & Fuels*, 22(6), 4125-4132.
- [84] Cao, Y., Wang, Y., Riley, J. T., & Pan, W-P. (2006). A Novel Biomass Air Gasification Process for Producing Tar-Free Higher Heating Value Fuel Gas. *Fuel Processing Technology*, 87, 343-53.
- [85] Gao, C. (2010). CO-Gasification of Biomass with Coal and Oil sand Coke in a Drop Tube Furnace. (Master's thesis), University of Alberta.
- [86] Hernandez J. J., Aranda-Almansa, G., & Serrano, C. (2010). CO-Gasification of Biomass Wastes and Coal–Coke Blends in an Entrained flow Gasifier: An Experimental Study, *Energy Fuel*, 24, 2479-88.
- [87] Pinto, F., Franco, C., Lopes, H., André, R., Gulyurtlu, I., & Cabrita, I. (2005). Effect of Used Edible Oils in Coal Fluidised Bed Gasification. *Fuel*, 84, 2236-2247.
- [88] Pohorely, M., Vosecky, M., Hejdová, P., Puncochár, M., Skoblja, S., Staf, M., et al. (2006). Gasification of Coal and PET in Fluidized Bed Reactor. *Fuel*, 85, 2458-2468.
- [89] Aznar, M. P., Caballero, M. A., & Sancho, J. A. (2006). France's E- Plastic Waste Elimination by CO-Gasification with Coal and Biomass in Fluidized Bed with Air in Pilot Plant. *Fuel Processing Technology*, 87, 409-420.
- [90] Sjostrom, K., Chen, G., Yu, Q., Brage, C., & Rosen, C. (1999). Promoted Reactivity of Char in CO-Gasification of Biomass and Coal: Synergies in the Thermochemical Process. *Fuel*, 78, 1189-1194.
- [91] Lee, W. J., Kim, S. D., & Song, B.-H. (2002). Steam Gasification of an Australian Bituminous Coal in a Fluidized Bed. *Korean Journal of Chemical Engineering*, 19, 1091-1096.
- [92] Lapuerta, M., Hernández, J. J., Pazo, A., & López, J. (2008). Gasification and CO-Gasification of Biomass Wastes: Effect of the Biomass Origin and the Gasifier Operating Conditions. *Fuel Processing Technology*, 89, 828-837.
- [93] Asadullah, M., Ito, S.-I., Kunimori, K., & Tomishige, K. (2002). Role of Catalyst and Its Fluidization in the Catalytic Gasification of Biomass to Syngas at Low Temperature. *Industrial & Engineering Chemistry Research*, 41, 4567-4575.
- [94] Seo, M. W., Goo, J. H., Kim, S. D., Lee, S. H., & Choi, Y. C. (2010). Gasification Characteristics of Coal/Biomass Blend in a Dual Circulating Fluidized Bed Reactor. *Energy Fuel*, 24, 3108-3118.
- [95] Kim, Y. J., Lee, S. H., & Kim, S. D. (2001). Coal Gasification Characteristics in a Downer Reactor. *Fuel*, 80, 1915-1922.

- [96] Kim, Y. J., Lee, J. M., & Kim, S.D. (1997). Coal Gasification Characteristics in an Internally Circulating Fluidized Bed With Draught Tube. *Fuel*, 76, 1067-1073.
- [97] Khadse, A., Parulekar, P., Aghalayam, P. & Ganesh, A. (2006). Equilibrium Model for Biomass Gasification. *Proceedings of the Advances in Energy Research Conference*, 106-112.
- [98] Syed, S., Janajreh, I., & Ghenai, C. (2012). Thermodynamics Equilibrium Analysis within the Entrained Flow Gasifier Environment. *International Journal of Thermal & Environmental Engineering*, 4(1), 47-54.
- [99] Ramanan, M. V., Lakshmanan, E., Sethumadhavan, R., & Renganarayanan, S. (2008). Modeling and Experimental Validation of Cashew Nut Shell Char Gasification Adopting Chemical Equilibrium Approach, *Energy Fuels*, 22(3), 2070-2078.
- [100] Li, X., Grace, J. R., Watkinson, A. P., Lim, C. J., & Ergüdenler, A. (2001). Equilibrium Modeling of Gasification: A Free Energy Minimization Approach and Its Application to a Circulating Fluidized Bed Coal Gasifier, *Fuel*, 80(2), 195-207.
- [101] Karmakar, M. K., & Datta, A. B. (2011). Generation of Hydrogen Rich Gas through Fluidized Bed Gasification of Biomass. *Bioresource Technology*, 102(2), 1907-1913. doi: <http://dx.doi.org/10.1016/j.biortech.2010.08.015>
- [102] Martínez, J. D., Silva Lora, E. E., Andrade, R. V., & Jaén, R. L. (2011). Experimental Study on Biomass Gasification in a Double Air Stage Downdraft Reactor. *Biomass and Bioenergy*, 35(8), 3465-3480. doi: <http://dx.doi.org/10.1016/j.biombioe.2011.04.049>
- [103] Acharya, B., Dutta, A., & Basu, P. (2010). An Investigation into Steam Gasification of biomass for Hydrogen Enriched Gas Production in Presence of CaO. *International Journal of Hydrogen Energy*, 35(4), 1582-1589. doi: <http://dx.doi.org/10.1016/j.ijhydene.2009.11.109>
- [104] Jarungthammachote, S., & Dutta, A. (2008). Equilibrium Modeling of Gasification: Gibbs Free Energy Minimization Approach and Its Application to Spouted Bed and Spout-Fluid Bed Gasifiers. *Energy Conversion and Management*, 49(6), 1345-1356.
- [105] Vaezi, M., Passandideh-Fard, M., Moghiman, M., & Charmchi, M. (2011). Gasification of Heavy Fuel Oils: A Thermochemical Equilibrium Approach. *Fuel*, 90(2), 878-885.
- [106] Chen, C., Horio, M., & Kojima, T. (2000). Numerical Simulation of Entrained Flow Coal Gasifiers. Part I: Modeling of Coal Gasification in an Entrained Flow Gasifier. *Chemical Engineering Science*, 55(18), 386-3874.
- [107] Bockelie, M. J., Denison, M. K., Chen, Z, Linjewile, T., Senior, C. L., Sarofim, A. F., & Holt, N. (n.d.). *CFD Modeling for Entrained Flow Gasifiers*. Retrieved from reaction-eng.com
- [108] Watanabe, H., & Otaka, M. (2006). Numerical Simulation of Coal Gasification in Entrained Flow Coal Gasifier. *Fuel*, 85(12-13), 1935-1943.
- [109] Shi, S., Zitney, S. A., Shahnam, M., Syntat, M., & Rogers, W. A. (2006). Modelling Coal Gasification with CFD and Discrete Phase Method. *Journal of the Energy Institute*, 79(4), 217-221.

- [110] Fletcher, D., Haynes, B. S., Christo, F. C., & Joseph, S. D. (2000, March). A CFD Based Combustion Model of an Entrained Flow Biomass Gasifier. *Applied Mathematical Modelling*, 24(3), 165-182.
- [111] Kumar M. (2011). *Multiscale CFD Simulation of Entrained Flow Gasification*. (Doctoral dissertation), Massachusetts Institute of Technology.
- [112] Hampp F., & Janajreh I. (2011). Development of a Drop Tube Reactor to Test and Assist a Sustainable Manufacturing Process. In Selinger, G., Kraishah, M., M., & Jawahir, I. S. (eds). *Advances in Sustainable Engineering* (141-148). Berlin: Springer.
- [113] Talab, I., Al-Nahari, Z., Qudaih, R., & Janajreh, I. (2010). Numerical Modeling of Coal Tire-Shred Co-Gasification. *Jordan Journal of Mechanical and Industrial Engineering*, 4(1), 155-162.
- [114] Janajreh, I., Talab, I., & Qudaih, R. (2009). Numerical Simulation of the Flow inside the Entrained Flow Gasifier. *Proceedings of 2009 US-EU-China Thermophysics Conference—Renewable Energy*.
- [115] Janajreh I., & Al Shrah, M. (2013). Numerical and Experimental Investigation of Downdraft Gasification of Wood Chips. *Energy Conversion and Management*, 65, 783-792.
- [116] Sun, Z., Dai, Z., Zhou, Z., Guo, Q., & Yu, G. (2012). Numerical Simulation of Industrial Opposed Multiburner Coal–Water Slurry Entrained Flow Gasifier. *Industrial & Engineering Chemistry Research*, 51(6), 2560-2569. doi: 10.1021/ie201542q
- [117] Luan, Y.-T., Chyou, Y.-P., & Wang, T. (2013). Numerical Analysis of Gasification Performance via Finite-Rate Model in a Cross-Type Two-Stage Gasifier. *International Journal of Heat and Mass Transfer*, 57(2), 558-566. doi: <http://dx.doi.org/10.1016/j.ijheatmasstransfer.2012.10.026>
- [118] Xie, J., Zhong, W., & Jin, B. (2014). LES-Lagrangian Modelling on Gasification of Combustible Solid Waste in a Spouted Bed. *The Canadian Journal of Chemical Engineering*, 92(7), 1325-1333. doi: 10.1002/cjce.21941

Biographies

ISAM JANAJREH is currently an associate mechanical engineering professor and the director of the Waste To Energy Lab at the Masdar Institute. He is an internationally recognized expert in the area of waste to energy particularly in the feedstock characterization thermochemical pathways, including gasification and pyrolysis. He has authored more than 80 publications in the subject and appeared in over 80 conferences. Dr. Isam Janajreh may be reached at ijanajreh@masdar.ac.ae.

IDOWU ADEYEMI is currently a Ph.D. candidate at Masdar Institute. He earned his M.S in Mechanical Engineering, 2014, from Masdar Institute; Idowu is part of the waste management group of Dr. Janajreh; he is well versed in both the experimental and the simulation of feedstock gasification. Mr. Idowu can be reached at iadeyemi@masdar.ac.ae.